Article

Less cytotoxic protoflavones as antiviral agents: protoapigenone 1′-*O*-isopropyl ether shows improved selectivity against the Epstein-Barr virus lytic cycle

Máté Vágvölgyi [1], Gábor Girst [1,2], Norbert Kúsz [1], Sándor B. Ötvös [2,3], Ferenc Fülöp [2,3], Judit Hohmann [1,4], Jean-Yves Servais [5], Carole Seguin-Devaux [5], Fang-Rong Chang [6], Hao Chen [7], Li-Kwan Chang [7], and Attila Hunyadi [1,4,*]

[1] Institute of Pharmacognosy, Interdisciplinary Excellence Centre, University of Szeged, 6720 Szeged, Hungary; vagvolgyi.mate@pharm.u-szeged.hu (M.V.); girst.gabor@pharmacognosy.hu (G.G.); kusz.norbert@pharm.u-szeged.hu (N.K.); hohmann@pharm.u-szeged.hu (J.H.)

[2] Institute of Pharmaceutical Chemistry, University of Szeged, 6720 Szeged, Hungary; otvossandor@pharm.u-szeged.hu (S.B.Ö.); fulop@pharm.u-szeged.hu (F.F.)

[3] MTA-SZTE Stereochemistry Research Group, Hungarian Academy of Sciences, 6720 Szeged, Hungary

[4] Interdisciplinary Centre for Natural Products, University of Szeged, 6720 Szeged, Hungary

[5] Department of Infection and Immunity, Luxembourg Institute of Health, 29 rue Henri Koch, L-4354 Esch-sur-Alzette, Luxemburg; Jean-Yves.Servais@lih.lu (J.-Y.S.); Carole.Devaux@lih.lu (C.S.-D.)

[6] Graduate Institute of Natural Products, Kaohsiung Medical University, Kaohsiung 807, Taiwan; aaronfrc@kmu.edu.tw

[7] Department of Biochemical Science and Technology, College of Life Science, National Taiwan University, Taipei City, Taiwan; b05b02041@ntu.edu.tw (H.C.); changlk@ntu.edu.tw

* Correspondence: hunyadi.a@pharm.u-szeged.hu; Tel.: +36-62-546-456

Abstract: Protoflavones, a rare group of natural flavonoids with a non-aromatic B-ring, are best known of their antitumor properties. The protoflavone B-ring is a versatile moiety that may be explored for other pharmacological purposes, but common cytotoxicity of these compounds is a limitation to such efforts. Protoapigenone was previously found to be active against the lytic cycle of Epstein-Barr virus (EBV). Further, the 5-hydroxyflavone moiety is a known pharmacophore against HIV-integrase. The aim of this work was to prepare a series of less cytotoxic protoflavone analogs, and to study their antiviral activity against HIV and EBV. Twenty-seven compounds including 18 new derivatives were prepared from apigenin through oxidative de-aromatization and subsequent continuous-flow hydrogenation, deuteration, and/or 4′-oxime formation. One compound was active against HIV at the micromolar range, and 3 compounds showed significant activity against the EBV lytic cycle at the medium-low nanomolar range. Among these, protoapigenone 1′-*O*-isopropyl ether (**6**) was identified as a promising lead due to its 73-times selectivity of its antiviral over its cytotoxic effect, which exceeds that of protoapigenone by 2.4-times. Our results open new opportunities to design new, potent and safe anti-EBV agents based on the natural protoflavone moiety.

Keywords: natural product; drug discovery; protoflavonoid; continuous-flow chemistry; oxime; antitumor; antiviral; Epstein-Barr virus; lytic cycle

1. Introduction

Protoflavonoids represent a relatively rare, naturally occurring group among natural flavonoids, possessing a non-aromatic B-ring and a hydroxyl function at C-1′. This unique structural moiety can appear in various forms, it is most typically a symmetric *p*-quinol dienone that may be partially or fully saturated, as shown by the examples of some natural protoflavones in Figure 1 [1].

Many protoflavones are known for their potent anticancer activity, and until now, this bioactivity of this compound family is by far the most deeply investigated. Protoflavones are known

to be cytotoxic on a wide range of cancer cell lines *in vitro*, and some protoflavones can selectively kill multi-drug resistant cancer cell lines adapted to chemotherapeutics [2,3]. Some protoflavones e.g. protoapigenone were also tested *in vivo* and were also found active against a variety of tumor xenograft models [1]. A particularly interesting property of protoapigenone is that it is a potent inhibitor of ATR-mediated activation of checkpoint kinase 1 (Chk1) [4], a DNA damage response mechanism that is an emerging antitumor target in the focus of several currently ongoing clinical trials [5].

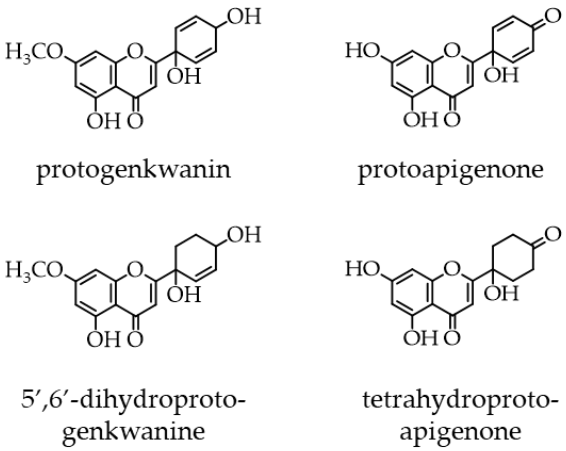

Figure 1: Examples of natural protoflavones with different moieties in their B-ring. A symmetric dienone structure, as in protoapigenone, is prerequisite of a strong cytotoxic activity.

From the available structure-activity relationships obtained from synthetic [6] and semi-synthetic [7] analogs, it is known that *a*) presence of a symmetric dienone with a non-substituted *p*-quinol B-ring is essential for a strong cytotoxic effect [8], and *b*) the introduction of a longer non-branching (e.g. butyl) alkyl substituent at the 1′-OH can further enhance cytotoxicity against some cell lines, while a branching alkyl substituent (e.g. isopropyl) strongly decreases it. It is also worth noting that a 1′-*O*-alkyl substitution results in a chemically much more stable B-ring as compared to the non-substituted p-quinol [7].

Possible uses of protoflavonoids may, however, exceed their antitumor potential. The non-aromatic B-ring containing an sp^3 carbon at C-1′ makes the 3D structure of these compounds very unique among flavonoids. This may lead to a versatile pharmacology that is hardly explored. Previously, we identified protoapigenone 1′-*O*-propargyl ether as the first non-planar flavonoid that can exert a potent inhibitory effect on xanthine oxidase, a pro-oxidant enzyme involved in many chronic diseases [9]. In addition to this, we found that protoapigenone exerts antiviral effect against the Epstein-Barr Virus (EBV) *in vitro* through inhibiting the expression of EBV lytic proteins [10]. These results suggest that the chemical space of protoflavones has still much to offer in bioactivities other than antitumor effect, while cytotoxicity itself certainly represents a limitation to explore this.

To overcome this limitation, we recently reported a method for the highly selective saturation of the protoflavone B ring by means of continuous flow hydrogenation under mild reaction conditions. This allowed us to obtain the rare, naturally occurring tetrahydroprotoflavone moiety, while also providing an effective tool to eliminate the cytotoxicity of the derivatives [11].

The aim of our current work was to further explore the antiviral potential of protoflavonoids by preparing a series of less cytotoxic derivatives, and to test them against EBV and, considering the antiretroviral activity of various other types of flavonoids [12-14], also against HIV.

2. Results and Discussion

2.1. Synthesis of B-ring modified protoapigenone analogs

First, we prepared 1′-*O*-alkyl substituted protoapigenone derivatives from apigenin (**1**), following our previously described procedure [7]. Oxidative dearomatization of the B-ring of

apigenin was achieved by a hypervalent iodine reagent, [bis(trifluoroacetoxy)iodo]benzene, and the solvent was 10% v/v of water or alcohol in acetonitrile depending on the substituent to be coupled at C-1′. This allowed us to obtain compounds **2**-**8** as potential intermediates for further transformations, among which **6** was already a compound of interest for this study due to its very weak cytotoxicity as compared to the others.

As detailed above, the function dominantly responsible for the cytotoxicity of protoflavones is the symmetric dienone moiety on the B-ring, conferring pro-oxidant and Micheal-acceptor properties to the compound. Considering this, we employed two different targeted synthetic strategies to eliminate cytotoxicity: i) saturation of the double bonds through hydrogenation or deuteration, and ii) substituting the 4′-oxo group with an oxime function. Synthetic routes are shown in Scheme 1.

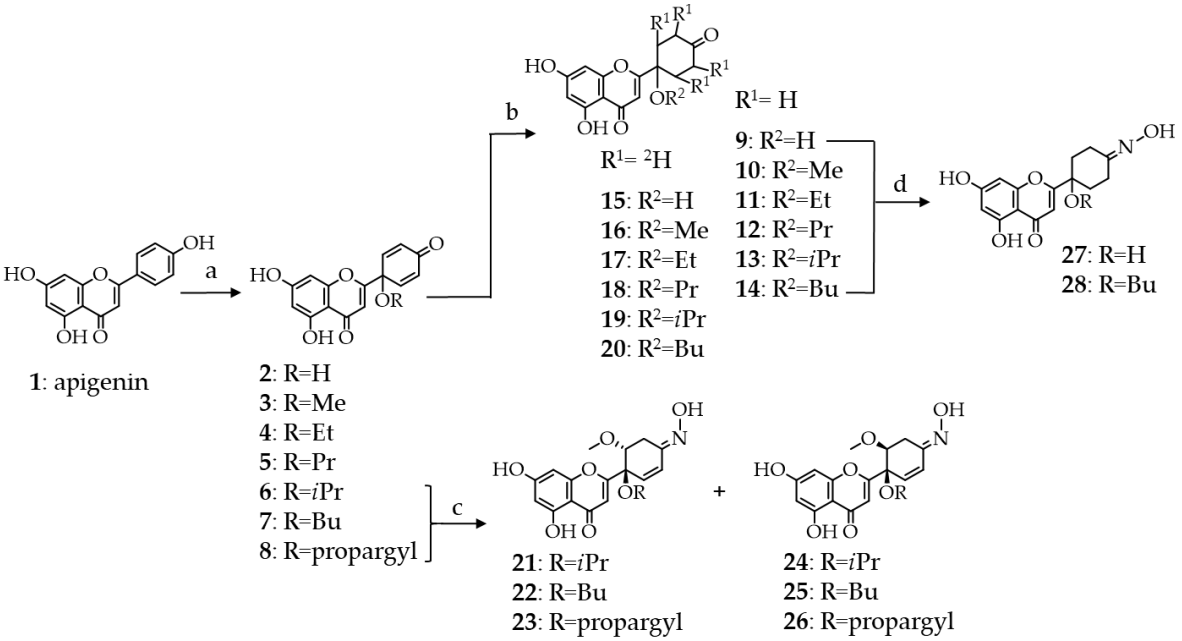

Scheme 1. Semi-synthetic routes employed for the preparation of tetrahydro-, tetradeutero- or 4′-oxime analogs of protoapigenone and its 1′-*O*-alkyl ether derivatives. Oxime derivatives **21-28** were obtained as racemates, however, for simplicity only one enantiomer is shown. *Reaction conditions:* a) CH_3CN/ROH - 9:1, PIFA (2 equiv.), 80°C, 1 h; b) H-Cube®, **9**-**14**: H_2, 5% Pd/C or **15**-**20**: D_2, 5% Pd/$BaSO_4$; c) $NH_2OH{\cdot}HCl$ (3 equiv.), MeOH, reflux, 24 h; d) $NH_2OH{\cdot}HCl$ (4 equiv.), MeOH, reflux, 3 h.

The hydrogenation of protoflavonoids' dienone moiety may result various products. Following our previously published procedure, saturation of the protoflavone B-ring was achieved with high selectivity under mild reaction conditions utilizing a modified H-cube® continuous flow hydrogenation reactor [11]. As compared to traditional batch hydrogenation, employing this device has several advantages, i.e. the ease of handling of the explosive gas, precise control over the reaction conditions, instrumentally controlled gas pressure, sustainability and safe applicability. During this process, hydrogen gas was generated *in situ* in an electrolytic, high purity water fueled cell, from which it was forwarded to interact with the substrate's solution. The mixture was then passed through a stainless-steel tube filled with the catalyst, where the triphasic reaction took place. During each transformation, the catalyst bed was placed in a thermostat for the aim to retain the temperature. Products of the reactions were collected into glass vials and, following evaporation, RP-HPLC purification was applied to obtain tetrahydroprotoapigenone analogs **9**-**14** in high purity (Scheme 1).

Deuterium is applied in organic chemistry for several purposes. It is employed as a tracer in studies that aim to follow reaction routes or as a reference to determine the influence of isotope effects on the development of a reaction during kinetic studies. Isotope labeling is a technique with versatile continuously developing applications, that include pharmacological utilization *via* metabolomics as well. Importance of deuterium in isotope labeling is increasing as new applications emerge [15,16].

Deuterium can also be of potential interest in terms of drug discovery since it can significantly influence bioactivity of a compound due to the so-called isotope effect [17,18]. Several methods are available for the synthetic preparation of deuterium containing compounds. The conventional batch synthesis of deuterated molecules suffers from similar drawbacks as hydrogenation, such as lack of sustainability and the low purity and high price of D_2 gas. Therefore, in this current work, we used a previously established continuous flow method [19-21], during which the required deuterium gas was generated from high purity D_2O in situ with H-Cube®. To ensure that no hydrogen-deuterium exchange occurs during the transformation, the reaction was performed in an aprotic solvent, ethyl acetate. For the same reason, we chose barium sulfate as the catalyst carrier, since activated charcoal might contain protic contaminations on its surface. In all other aspects of the synthesis, we followed the same procedure as in the case of hydrogenation, to obtain tetradeuteroprotoapigenone derivatives **15-20** (Scheme 1).

Several studies underline that the preparation of flavonoid oxime derivatives can be a simple yet effective synthetic option to enhance certain biological effects of the parent compound, e. g. antimicrobial [22], antioxidant [23], and antitumor [24] properties. To further increase chemical and consequential pharmacological diversity, compounds with different B-ring saturation and/or 1′-*O*-substituents (**6**-**9** and **14**) were selected for the preparation of 4′-oximes (Scheme 1).

Our preliminary small-scale test reactions indicated that oxime formation of protoflavones is regioselective at the 4′-keto group, and under the synthetic conditions applied we did not observe the formation of 4-oxime nor 4,4′-dioxime side products. On the other hand, the solvent appeared to play a crucial role in the possible outcome of the transformation. Pyridine, ethanol and acetonitrile are probably among the most commonly used solvents in oxime synthesis. However, none of these worked in our case, and finally we found methanol as the best solvent for reacting protoflavones with hydroxylamine. Yields appeared to vary greatly depending on the substrate's concentration in the reaction solution, and we obtained the best yields with ca. 2-2.5 mg/mL concentrations; both lower and higher concentrations could significantly decrease efficiency of the transformation.

Regioselective transformation of the tetrahydroprotoflavone analogs **9** and **14** to their corresponding 4′-oximes **27** and **28** was straightforward. However, in case of protoflavones **6**-**8**, each transformation was accompanied by a regioselective Michael addition of methanol at C-2′, forming a methoxy group and saturating one of the double bonds to yield 2′-methoxy-2′3′-dihydroprotoapigenone 4′-oxime derivatives **21-26.** The orientation of the methoxy group was apparently random since the 1′,2′-*cis* and *trans* derivatives were formed in a ca. 1:1 ratio. When assigning the relative configuration of the 1′,2′-carbon atoms, we could not observe diagnostic NOESY cross-peaks between the 2′-methoxy and the 1′-*O*-alkyl substituents for any of these compounds. Therefore, *cis*-*trans* isomers were assigned based on the characteristic coupling constant patterns observed between H-2′ and H-3′a or H-3′b. To achieve this, structures were optimized by the MMFF94x force field in CCG-MOE, the H2′-C2′-C3′-H3′a and H2′-C2′-C3′-H3′b dihedral angles were measured, and theoretical ^{1}H-^{1}H ^{3}J coupling constants were calculated by means of the Bothner-By equation. The experimental coupling constants showed good agreements with the calculated values, unambiguously assigning compounds **21**-**23** as the 1′,2′-*trans*, and **24**-**26** as the 1′,2′-*cis* isomers. Nevertheless, while each compound was obtained as racemate, the newly formed oxime took a defined orientation in all of them. This suggests that the solvent addition took place to an intermediate of the reaction in a way that it determined the final orientation of the oxime. Since this way the exact data of the Δδ syn-anti parameters were not available, we considered compounds **27** and **28** as internal references, which provided us with the chemical shifts for both neighbouring methylenes of the oxime. In these compounds, C-3′ (syn) and C-5′ (anti) gave ^{13}C NMR chemical shifts at ca. 18.8 and 26.2 ppm, respectively. The ^{13}C NMR signals of the 3′-CH_2 moieties of compounds **21**-**26** appeared within the range of 22.7-23.7 ppm, which, also taking into account the effect of the electron-rich neighbouring OCH_3 group, strongly suggests that the oxime is present in *E*-orientation in each of these compounds.

2.2. Biological activities

2.2.1. Antiretroviral activity

Compounds **2**, **6**-**14** and **21**-**28** were tested against HIV-1 using a pseudotype virus assay allowing only one cycle of viral replication and being more sensitive for compounds targeting the early steps of HIV replication such as reverse transcription and integration [25]. Tetrahydroprotoapigenone (**9**) was found to inhibit viral infection by ca. 50% at the non-cytotoxic concentration of 100 μM (see Supplementary Figure S55). While this represents a rather weak activity, it may still be of interest since this compound was not cytotoxic on the host cells at as high as 500 μM concentration.

2.2.2. Antiviral activity against EBV

Compounds **2** and **6**-**28** were tested for their activity on the EBV lytic cycle. To assess this, P3HR1 cells were treated with sodium butyrate and TPA for 24 h. As expected, lytic protein Rta was expressed after lytic induction. As a first screening, cells were treated with protoapigenone (**2**), used as a positive control, or compounds **6**-**28** at the induction of lytic cycle for 24 h. The concentration selected for screening was 0.25 μM, where protoapigenone (**2**) was previously found to exert a strong activity [10]. The results indicated that three of the analogs, **6**, **7**, and **8** can inhibit EBV lytic cycle at this concentration. These compounds were then tested for the dose dependency of their effect on the expression of Rta; results are shown in Figure 2.

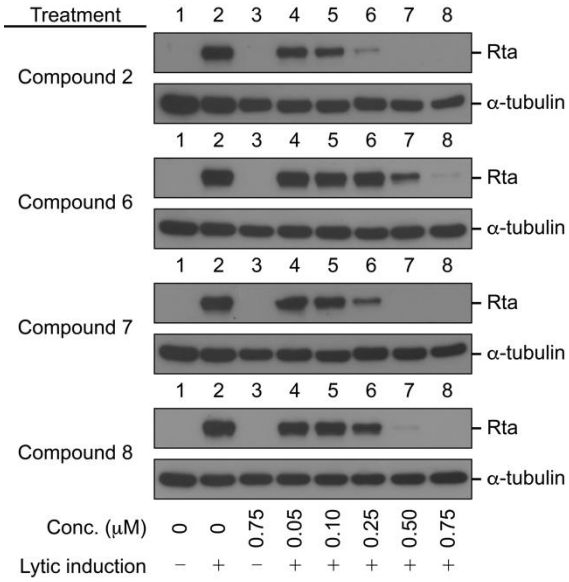

Figure 2. Inhibition of the expression of EBV Rta by protoapigenone (**2**) and its analogs **6**-**8**. Cells were treated with the compounds at the time of lytic induction with SB and TPA. Cell lysates were harvested at 24 h after lytic induction. Proteins in the lysate were detected by immunoblotting using anti-Rta and anti-α-tubulin antibodies. Calculated IC_{50} values for **2**, **6**, **7** and **8** were 0.127, 0.467, 0.208, and 0.285 μM, respectively.

We found that, similarly to protoapigenone (**2**), compounds **6**, **7** and **8** also caused a marked reduction in Rta levels at 0.50, 0.25, and 0.50 μM, respectively, and the IC_{50} values were calculated as 0.467, 0.208, and 0.285 μM, respectively. The positive control protoapigenone (**2**) acted with an IC_{50} value of 0.127 μM that was in good agreement with our previous findings [10]. Subsequently, we conducted MTT assay to evaluate the cytotoxicity of these compounds to P3HR1 cells; results are shown in Figure 3.

As expected from our previously published structure-activity relationship (SAR) study on the effect of 1′-*O*-alkyl substituents on the cytotoxic activity of protoflavones [7], compounds **7** and **8**

Preprints (www.preprints.org) | NOT PEER-REVIEWED | Posted: 4 December 2019 doi:10.20944/preprints201912.0049.v1

Peer-reviewed version available at Int. J. Mol. Sci. 2019, 20, 6269; doi:10.3390/ijms20246269

were similarly active as protoapigenone (**2**), and the isopropyl-ether derivative **6** was much weaker in this regard. Selectivity of the anti-EBV vs. cytotoxic effect of these compounds, expressed as a ratio of the corresponding IC_{50} values, could therefore be calculated as follows: **2** (30.1), **6** (73.0), **7** (9.80), and **8** (17.3). This means that compound **6** demonstrated a relevant, ca. 2.6-times increase in selectivity as compared to protoapigenone. It is also worth noting that by appropriate modifications of the B-ring it was also found possible to shift the bioactivity profile of protoflavones to the other direction. Compound **7** was less effective against EBV and more cytotoxic than protoapigenone, i.e. ca. 3-times less selective in this regard. Therefore, SAR of protoflavonoids may be explored towards various therapeutic targets, and this is certainly a need to evaluate their real value concerning drug discovery.

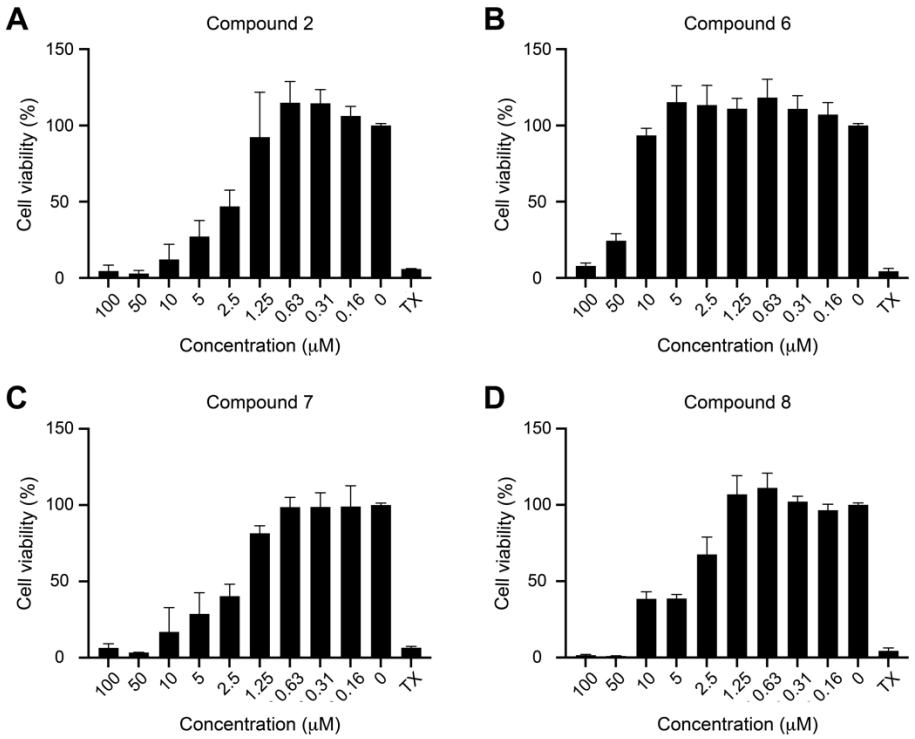

Figure 3. Cytotoxicity of protoapigenone and its analogs to P3HR1 cells. Cells were cultured for 24 h in a medium containing protoapigenone (**2**) or compounds **6**-**8**. Cell viability was evaluated by using MTT assay. Cells treated with 1% Triton X-100 (TX) were used as a positive control. The experiment was performed twice, and each sample involved in the experiment was prepared in duplicate. Error bars represent SD. Calculated IC_{50} values for compounds **2**, **6**, **7** and **8** were 3.86, 34.12, 2.04 and 4.93 μM, respectively.

4. Materials and Methods

4.1. Synthesis and chromatographic purification

Reagents were purchased from Sigma (Merck KGaA, Germany), and solvents were obtained from Macron Fine Chemicals (Avantor Performance Materials, USA). Reactions were monitored by TLC on Kieselgel $60F_{254}$ silica plates purchased from Merck (Merck, Germany), and characteristic spots of compounds were examined under UV illumination at 254 and 366 nm. Depending on the complexity of protoflavone product mixtures, chromatographic purification of components was carried out in one or two steps. For flash chromatography, a CombiFlash® Rf+ Lumen apparatus (TELEDYNE Isco, USA) was utilized that was equipped with ELS and diode array detectors. Components were separated on commercially available RediSep NP-silica flash columns (TELEDYNE Isco, USA) or manually filled polyamide columns. Mobile phase eluents consisted of mixtures of *n*-hexane – ethyl acetate or dichloromethane – methanol, modified according to the polarity of the analytes. To determine the composition of sample mixtures or to evaluate the purity of compounds, RP-HPLC analysis was performed on a Kinetex XB-C18 250 x 4.6 mm 5 μm or a

Kinetex Biphenyl 250 x 4.6 mm 5 µm column (Phenomenex Inc., USA) at 1 ml/min flow rate, using a dual pump (PU-2080) Jasco HPLC instrument (Jasco Analytical Instruments, Japan) that was equipped with an MD-2010 Plus PDA detector to collect data in a detection range of 210-400 nm. For preparative purposes, an Armen Spot Prep II integrated HPLC purification system (Gilson, USA) with dual-wavelength detection was applied, operating at 230 and 300 nm. Preparative separations were performed on the corresponding Kinetex XB-C18 or Biphenyl 250 x 21.2 mm 5 µm columns with adequately chosen eluents of acetonitrile – water, and the flow rates were 15 ml/min.

4.1.1. Preparation of protoapigenone derivatives **2**-**8**.

Protoapigenone and its 1′-*O*-alkyl ether analogs were synthesized following our previously described procedures [7]. Briefly, apigenin (1 mg/mL) was dissolved in a 9:1 v/v ratio mixture of acetonitrile and H_2O or the alcohol to be coupled at C-1′. Under stirring, 2 equivalents of [bis(trifluoroacetoxy)iodo]benzene was added slowly to the solution and the reaction was left to develop for 1 hour at 80 °C. After completion, solvent was evaporated on a rotary evaporator and the residue was purified by flash chromatography allowing to obtain the corresponding protoflavones in pure form.

4.1.2. Preparation of tetrahydroprotoapigenone derivatives **9**-**14**.

Selective hydrogenation of protoflavones was carried out based on our previous strategy [11] that relied on the application of an H-Cube® continuous flow hydrogenation system (ThalesNano Inc., Hungary). The applied catalyst cartridge was a stainless-steel column (internal dimensions: 50 mm × 4.6 mm) containing approximately 200 mg of 5% Pd/C catalyst. The cartridge was inserted into an external thermostat (Jetstream 2 plus, Jasco, Japan) set to 25 °C. To provide continuous stream, a standard HPLC pump (Well-Chrom K-120, Knauer GmbH, Germany) was used. In each case, flow rate was set to 1 ml/min, and 40 bar pressure was applied in the system.

For each reaction, 20 mg of the corresponding protoflavone was dissolved / suspended in 20 mL of HPLC grade ethyl acetate and homogenized by sonication. To ensure reproducibility, between each reaction, the catalyst bed was washed with the solvent for 15 minutes. Following transformations, preparative RP-HPLC was utilized for chromatographic purification.

4.1.3. Preparation of tetradeuteroprotoapigenone derivatives **15**-**20**.

Selective deuteration of the protoflavone B ring was performed similarly as described for hydrogenation with only slight modifications. In this case, approximately 400 mg of 5% $Pd/BaSO_4$ was used as a catalyst, and the reservoir of the instrument was filled up with high purity heavy water (D_2O). The obtained compounds **15**-**20** were purified by preparative RP-HPLC.

4.1.4. Preparation of protoflavone 4′-oxime derivatives **21**-**26**.

An aliquot of 150 mg of compound **6**, **7**, or **8** was dissolved in methanol in a concentration of 2.5 mg/mL (50 mL). Following this, 3 equivalents of hydroxylamine hydrochloride were added to the solution, and the mixture was refluxed for 24 h at 70 °C. Silica gel (3-5 g) was added to the solution, and the solvent was evaporated to prepare for dry loading separation. The dried residue was applied to flash chromatography, and products were pre-purified by a gradient separation program of *n*-hexane/ethyl acetate – 100:0 (v/v) gradually increasing to 10:90 in 15 min. Following this, cis- and trans-isomeric racemate pairs (**21** and **24**, **22** and **25**, **23** and **26**, respectively) were separated by means of preparative RP-HPLC to obtain racemates **21**-**26**.

4.1.5. Preparation of tetrahydroprotoflavone 4′-oxime derivatives **27**-**28**.

An aliquot of 60 mg of tetrahydroprotoflavone **9** or **14** was dissolved in methanol in a concentration of 2.5 mg/mL (25 mL). 4 equivalents of hydroxylamine hydrochloride were added to the mixture, and the solution was stirred at 70 °C for 3 hours. Following this, solvent was evaporated on a rotary evaporator and brine (40 mL) was added to the residue. Extraction was performed with

EtOAc (3x40 mL), and then the organic fractions were combined and dried over Na_2SO_4. Drying agent was removed through filtration, and the solution was evaporated under reduced pressure. Eventually, preparative RP-HPLC was applied to obtain oxime derivatives **27** and **28**.

4.2. Structure elucidation

The compounds were characterized by NMR and MS techniques. NMR spectra were recorded at 25 °C on a Bruker Avance DRX 400 MHz (Bruker Co., USA) or on a Bruker Avance NEO 500 MHz spectrometer equipped with a Prodigy BBO 5 mm CryoProbe with the use of TMS as an internal standard. Typically, 5-10 mg of the corresponding protoflavone was dissolved in DMSO-d_6 and transferred to NMR tubes for recording spectra. Data report and spectra analysis were carried out with MestReNova v6.0.2-5475 software (Mestrelab Research S.L., Spain). ^{1}H and ^{13}C NMR chemical shifts are listed below; residual hydrogen signals of the B-rings of deuterated compounds **15**-**20** are marked with an asterisk. Mass spectra were recorded on an API 2000 triple quadrupole tandem mass spectrometer (AB SCIEX, USA) equipped with ESI ion source that was used in the negative ionization mode.

Compound **10**: Pale yellow solid, Isolated yield: 25.2% (5.1 mg); RP-HPLC purity: 97%. ^{1}H NMR (500 MHz, DMSO-d_6): 12.65 (1H, s), 10.93 (1H, br s), 6.39 (1H, d, J = 1.9 Hz), 6.34 (1H, s), 6.20 (1H, d, J = 1.9 Hz), 3.22 (3H, s), 2.56 (2H, m), 2.35 (2H, m), 2.18–2.22 (4H, m). ^{13}C NMR (125 MHz, DMSO-d_6): 208.9, 181.7, 168.9, 164.5, 161.4, 157.8, 107.5, 103.9, 99.0, 94.1, 75.7, 51.0, 2 x 35.8, 2 x 30.8. ESI-MS (m/z): 303.4 $[M-H]^-$.

Compound **11**: Pale yellow solid, Isolated yield: 70.5% (15.5 mg); RP-HPLC purity: 98%. ^{1}H NMR (500 MHz, DMSO-d_6): 12.66 (1H, s), 10.94 (1H, br s), 6.39 (1H, d, J = 1.9 Hz), 6.32 (1H, s), 6.20 (1H, d, J = 1.9 Hz), 3.40 (2H, q, J = 6.9 Hz), 2.55 (2H, m), 2.34 (2H, m), 2.16–2.22 (4H, m), 1.16 (3H, t, J = 6.9 Hz). ^{13}C NMR (125 MHz, DMSO-d_6): 209.0, 181.7, 169.6, 164.5, 161.4, 157.7, 107.1, 103.8, 99.0, 94.0, 75.5, 58.6, 2 x 35.9, 2 x 31.3, 15.5. ESI-MS (m/z): 317.7 $[M-H]^-$.

Compound **12**: Pale brown solid, Isolated yield: 30.1% (6.1 mg); RP-HPLC purity: 99%. ^{1}H NMR (500 MHz, DMSO-d_6): 12.65 (1H, s), 10.97 (1H, br s), 6.38 (1H, d, J = 1.9 Hz), 6.32 (1H, s), 6.20 (1H, d, J = 1.9 Hz), 3.30 (2H, t, J = 6.4 Hz), 2.56 (2H, m), 2.36 (2H, m), 2.16–2.22 (4H, m), 1.55 (2H, m), 0.89 (3H, t, J = 7.4 Hz). ^{13}C NMR (125 MHz, DMSO-d_6): 209.0, 181.7, 169.3, 164.6, 161.4, 157.7, 107.3, 103.8, 99.0, 94.0, 75.2, 64.5, 2 x 35.9, 2 x 31.2, 22.8, 10.7. ESI-MS (m/z): 331.3 $[M-H]^-$.

Compound **13**: Pale yellow solid, Isolated yield: 44% (8.9 mg); RP-HPLC purity: 99%. ^{1}H NMR (500 MHz, DMSO-d_6): 12.62 (1H, s), 10.99 (1H, br s), 6.42 (1H, s), 6.39 (1H, d, J = 1.9 Hz), 6.20 (1H, d, J = 1.9 Hz), 3.82 (1H, septet, J = 6.1 Hz), 2.55 (2H, m), 2.42 (2H, m), 2.13–2.21 (4H, m), 1.02 (6H, d, J = 6.1 Hz). ^{13}C NMR (125 MHz, DMSO-d_6): 209.2, 181.7, 169.0, 164.8, 161.4, 157.5, 108.0, 103.9, 99.1, 93.9, 75.0, 66.1, 2 x 36.1, 2 x 31.6, 2 x 24.0. ESI-MS (m/z): 331.4 $[M-H]^-$.

Compound **15**: Pale yellow solid, Isolated yield: 63.1% (12.6 mg); RP-HPLC purity: 98,9%. ^{1}H NMR (500 MHz, DMSO-d_6): 12.73 (1H, s), 6.41 (1H, s), 6.38 (1H, d, J = 1.9 Hz), 6.18 (1H, d, J = 1.9 Hz), 6.08 (1H, br s), 2 x 2.26* (d, J = 4.7 Hz), 2 x 2.17* (d, J = 4.7 Hz). ^{13}C NMR (125 MHz, DMSO-d_6): 209.6, 182.0, 174.3, 164.5, 161.4, 157.6, 104.7, 103.6, 98.9, 94.0, 70.2, 2 x 35.7, 2 x 33.7. ESI-MS (m/z): 293.5 $[M-H]^-$.

Compound **16**: White solid, Isolated yield: 40.5% (8.2 mg); RP-HPLC purity: 95%. ^{1}H NMR (500 MHz, DMSO-d_6): 12.65 (1H, s), 10.96 (1H, br s), 6.39 (1H, d, J = 1.9 Hz), 6.34 (1H, s), 6.20 (1H, d, J = 1.9 Hz), 3.21 (3H, s), 2.52* (br d, J = 6.1 Hz) 2.33* (br d, J = 6.1 Hz), 2 x 2.18* (m). ^{13}C NMR (125 MHz, DMSO-d_6): 209.1, 181.7, 168.9, 164.6, 161.4, 157.8, 107.6, 103.8, 99.0, 94.1, 75.7, 51.0, 2 x 35.4, 2 x 30.4. ESI-MS (m/z): 307.4 $[M-H]^-$.

Compound **17**: Pale pink solid, Isolated yield: 60.6% (12.1 mg); RP-HPLC purity: 96%. ^{1}H NMR (500 MHz, DMSO-d_6): 12.66 (1H, s), 10.94 (1H, br s), 6.39 (1H, d, J = 1.9 Hz), 6.32 (1H, s), 6.21 (1H, d, J = 1.9 Hz), 3.40 (2H, q, J = 6.9 Hz), 2.54* (br d, J = 6.0 Hz), 2.32* (br d, J = 6.0 Hz), 2 x 2.17* (m), 1.16 (3H, t, J = 6.9 Hz). ^{13}C NMR (125 MHz, DMSO-d_6): 209.1, 181.7, 169.5, 164.6, 161.4, 157.7, 107.1, 103.8, 99.0, 94.0, 75.4, 58.6, 2 x 35.5, 2 x 30.9, 15.5. ESI-MS (m/z): 321.3 $[M-H]^-$.

Compound **18**: White solid, Isolated yield: 51.4% (10.4 mg); RP-HPLC purity: 98%. ^{1}H NMR (500 MHz, DMSO-d_6): 12.64 (1H, s), 10.97 (1H, br s), 6.38 (1H, d, J = 1.9 Hz), 6.32 (1H, s), 6.20 (1H, d, J = 1.9 Hz), 3.30 (2H, t, J = 6.3 Hz), 2.53* (br d, J = 6.1 Hz), 2.34* (br d, J = 6.1 Hz), 2 x 2.17* (m), 1.55 (2H, m), 0.88 (3H, t, J = 7.3 Hz). ^{13}C NMR (125 MHz, DMSO-d_6): 209.6, 182.1, 169.7, 165.1, 161.9, 158.2, 107.8, 104.3, 99.5, 94.5, 75.5, 64.9, 2 x 35.9, 2 x 31.3, 23.2, 11.1. ESI-MS (m/z): 335.5 $[M-H]^-$.

Compound **19**: White solid, Isolated yield: 55.8% (11.3 mg); RP-HPLC purity: 99%. ^{1}H NMR (500 MHz, DMSO-d_6): 12.62 (1H, s), 11.01 (1H, br s), 6.42 (1H, s), 6.39 (1H, d, J = 1.9 Hz), 6.21 (1H, d, J = 1.9 Hz), 3.81 (1H, septet, J = 6.1 Hz), 2.53* (br d, J = 5.9 Hz), 2.39* (br d, J = 5.9 Hz), 2.17* (m), 2.13* (m), 1.01 (6H, d, J = 6.1 Hz). ^{13}C NMR (125 MHz, DMSO-d_6): 209.4, 181.7, 169.0, 164.8, 161.4, 157.5, 108.0, 103.8, 99.1, 93.9, 75.0, 66.0, 2 x 35.7, 2 x 31.2, 2 x 24.0. ESI-MS (m/z): 335.5 $[M-H]^-$.

Compound **20**: White solid, Isolated yield: 73.5% (14.7 mg); RP-HPLC purity: 99%. ^{1}H NMR (500 MHz, DMSO-d_6): 12.64 (1H, s), 10.98 (1H, br s), 6.37 (1H, d, J = 1.7 Hz), 6.32 (1H, s), 6.19 (1H, d, J = 1.7 Hz), 3.33 (2H, overlap with H_2O signal, J = 5.7 Hz), 2.53* (br d, J = 6.1 Hz), 2.34* (br d, J = 6.1 Hz), 2 x 2.17* (m), 1.52 (2H, m), 1.36 (2H, m), 0.85 (3H, t, J = 7.4 Hz). ^{13}C NMR (125 MHz, DMSO-d_6): 209.2, 181.6, 169.3, 164.7, 161.4, 157.7, 107.4, 103.8, 99.1, 94.0, 75.1, 62.5, 2 x 35.5, 31.6, 2 x 30.8, 18.9, 13.8. ESI-MS (m/z): 349.8 $[M-H]^-$.

Racemate **21**: Pale brown solid; Isolated yield: 24.3% (41.67 mg); RP-HPLC purity at 241 nm: 99.5%. ^{1}H NMR (500 MHz, DMSO-d_6): 12.69 (1H, s), 11.45 (1H, s), 6.50 (1H, d, J = 10.1 Hz), 6.35 (1H, s), 6.34 (1H, d, J = 1.8 Hz), 6.32 (1H, d, J = 10.1 Hz), 6.20 (1H, d, J = 1.8 Hz), 3.91 (1H, septet, J = 6.1 Hz), 3.71 (1H, dd, J = 10.0 and 4.4 Hz), 3.18 (3H, s), 3.01 (1H, dd, J = 16.7 and 4.4 Hz), 2.43 (1H, dd, J = 16.7 and 10.0 Hz), 1.11 (3H, d, J = 6.1 Hz), 1.07 (3H, d, J = 6.1 Hz). ^{13}C NMR (125 MHz, DMSO-d_6): 181.5, 169.9, 164.6, 161.5, 157.6, 152.3, 130.1, 129.9, 108.4, 103.9, 99.1, 94.0, 79.0, 77.9, 67.6, 57.3, 24.03, 24.02, 23.6. ESI-MS (m/z): 374.7 $[M-H]^-$.

Racemate **22**: Pale brown solid; Isolated yield: 27.8% (47.43 mg); RP-HPLC purity at 247 nm: 99.9%. ^{1}H NMR (500 MHz, DMSO-d_6): 12.68 (1H, s), 11.43 (1H, br s), 6.48 (1H, d, J = 10.0 Hz), 6.33 (1H, d, J = 2.0 Hz), 6.29 (1H, d, J = 10.0 Hz), 6.25 (1H, s), 6.21 (1H, d, J = 2.0 Hz), 3.76 (1H, dd, J = 10.1 and 4.7 Hz), 3.43 (2H, m), 3.18 (3H, s), 3.03 (1H, dd, J = 16.8 and 4.7 Hz), 2.45 (1H, dd, J = 16.8 and 10.2 Hz), 1.50 (2H, m), 1.32 (2H, m), 0.85 (3H, t, J = 7.4 Hz). ^{13}C NMR (125 MHz, DMSO-d_6): 181.4, 168.5, 164.5, 161.5, 157.8, 152.2, 130.1, 129.7, 108.2, 103.9, 99.1, 94.0, 78.6, 77.7, 64.1, 57.5, 31.8, 23.7, 18.8, 13.7. ESI-MS (m/z): 388.0 $[M-H]^-$.

Racemate **23**: Pale brown solid; Isolated yield: 25.1% (43.11 mg); RP-HPLC purity at 248 nm: 99.8%. ^{1}H NMR (500 MHz, DMSO-d_6): 12.67 (1H, s), 11.52 (1H, s), 6.52 (1H, d, J = 10.0 Hz), 6.33 (1H, d, J = 1.9 Hz), 6.32 (1H, s), 6.29 (1H, d, J = 10.0 Hz), 6.21 (1H, d, J = 1.9 Hz), 4.27 (1H, dd, J = 15.7 and 2.3 Hz), 4.18 (1H, dd, J = 15.7 and 2.3 Hz), 3.80 (1H, dd, J = 10.2 and 4.7 Hz), 3.46 (1H, t, J = 2.3 Hz), 3.18 (3H, s), 3.07 (1H, dd, J = 16.7 and 4.7 Hz), 2.43 (1H, dd, J = 16.7 and 10.2 Hz). ^{13}C NMR (125 MHz, DMSO-d_6): 181.5, 167.8, 164.5, 161.5, 157.7, 152.1, 130.8, 128.7, 108.4, 104.0, 99.1, 94.1, 80.5, 78.33, 78.31, 77.5, 57.4, 53.3, 23.7. ESI-MS (m/z): 370.3 $[M-H]^-$.

Racemate **24**: Pale brown solid; Isolated yield: 29.6% (50.76 mg); RP-HPLC purity at 246 nm: 97.3%. ^{1}H NMR (500 MHz, DMSO-d_6): 12.66 (1H, s), 11.38 (1H, s), 6.47 (3H, m, overlapping signals), 6.36 (1H, d, J = 1.9 Hz), 6.21 (1H, d, J = 1.9 Hz), 3.84–3.92 (2H, m, overlapping signals), 3.12 (1H, dd, J = 12.3 and 4.2 Hz), 3.10 (3H, s), 2.52 (1H, dd, J = 3.4 Hz; partially overlapped with DMSO signal),

1.04 (3H, d, *J* = 6.1 Hz), 0.97 (3H, d, *J* = 6.1 Hz). ^{13}C NMR (125 MHz, DMSO-d_6): 181.5, 168.7, 164.7, 161.5, 157.4, 151.1, 130.1, 127.3, 108.9, 103.9, 99.1, 93.8, 78.2, 76.6, 66.6, 56.9, 24.4, 23.8, 22.7. ESI-MS (m/z): 374.7 $[M-H]^-$.

Racemate **25**: Pale brown solid; Isolated yield: 33.2% (56.64 mg); RP-HPLC purity at 247 nm: 99.7%. ^{1}H NMR (500 MHz, DMSO-d_6): 12.65 (1H, br s), 11.39 (1H, s), 10.92 (1H, br s), 6.48 (1H, d, *J* = 10.3 Hz), 6.42 (1H, s), 6.36 (1H, d, *J* = 10.3 Hz), 6.32 (1H, d, *J* = 2.1 Hz), 6.21 (1H, d, *J* = 2.1 Hz), 3.90 (1H, br t, *J* = 4.3 Hz), 3.45 (1H, m), 3.28 (1H, m), 3.15 (3H, s), 3.02 (1H, dd, *J* = 17.4 and 5.1 Hz), 2.61 (1H, dd, *J* = 17.4 and 3.9 Hz), 1.45 (2H, m), 1.30 (2H, m), 0.82 (3H, t, *J* = 7.4 Hz). ^{13}C NMR (125 MHz, DMSO-d_6): 181.5, 168.0, 164.5, 161.5, 157.5, 151.1, 130.1, 127.6, 108.7, 103.9, 99.1, 93.8, 78.0, 77.3, 62.8, 57.2, 31.6, 23.3, 18.7, 13.6. ESI-MS (m/z): 388.2 $[M-H]^-$.

Racemate **26**: Pale brown solid; Isolated yield: 31.8% (54.62 mg); RP-HPLC purity at 248 nm: 97.3%. ^{1}H NMR (500 MHz, DMSO-d_6): 12.65 (1H, s), 11.48 (1H, s), 6.53 (1H, d, *J* = 10.3 Hz), 6.44 (1H, s), 6.40 (1H, d, *J* = 10.3 Hz), 6.34 (1H, d, *J* = 1.9 Hz), 6.20 (1H, d, *J* = 1.9 Hz), 4.21 (1H, dd, *J* = 15.8 and 2.3 Hz), 4.15 (1H, dd, *J* = 15.8 and 2.3 Hz), 3.93 (1H, dd, *J* = 4.6 and 3.6 Hz), 3.39 (1H, t, *J* = 2.3 Hz), 3.14 (3H, s), 3.04 (1H, dd, *J* = 17.4 and 4.6 Hz), 2.57 (1H, dd, *J* = 17.4 and 3.6 Hz). ^{13}C NMR (125 MHz, DMSO-d_6): 181.5, 167.1, 164.6, 161.5, 157.5, 151.0, 131.1, 126.0, 109.0, 104.0, 99.1, 93.9, 80.3, 77.9, 77.6, 77.4, 57.2, 52.1, 23.1. ESI-MS (m/z): 370.2 $[M-H]^-$.

Racemate **27**: Pale white solid; Isolated yield: 48.3% (30.5 mg); RP-HPLC purity at 247 nm: 96.1%. ^{1}H NMR (500 MHz, DMSO-d_6): 12.75 (1H, s), 10.34 (1H, s), 6.37 (1H, d, *J* = 1.9 Hz), 6.36 (1H, s), 6.18 (1H, d, *J* = 1.9 Hz), 5.84 (1H, br s), 3.08 (1H, br d, *J* = 14.2 Hz), 2.45 (1H, td, *J* = 13.4 and 4.9 Hz), 2.21 (1H, m), 2.06 (1H, m), 1.98 (1H, td, *J* = 12.9 and 4.6 Hz), 1.80–1.89 (3H, m, overlapping signals). ^{13}C NMR (125 MHz, DMSO-d_6): 182.1, 174.9, 164.4, 161.4, 157.6, 155.4, 104.5, 103.6, 98.9, 94.0, 71.2, 34.6, 33.3, 26.3, 18.8. ESI-MS (m/z): 304.4 $[M-H]^-$.

Racemate **28**: Pale white solid; Isolated yield: 42.1% (26.4 mg); RP-HPLC purity at 250 nm: 96.6%. ^{1}H NMR (500 MHz, DMSO-d_6): 12.66 (1H, s), 10.36 (1H, s), 6.38 (1H, d, *J* = 1.9 Hz), 6.27 (1H, s), 6.19 (1H, d, *J* = 1.9 Hz), 3.28 (2H, t, *J* = 6.1 Hz), 3.05 (1H, br d, *J* = 14.4 Hz), 2.33 (1H, td, *J* = 13.9 and 5.4 Hz), 2.16–2.23 (3H, m, overlapping signals), 1.98 (1H, td, *J* = 13.6 and 5.1 Hz), 1.87 (1H, td, *J* = 14.2 and 4.3 Hz), 1.78 (1H, td, *J* = 13.3 and 4.6 Hz), 1.49 (2H, m), 1.35 (2H, m), 0.84 (3H, t, *J* = 7.4 Hz). ^{13}C NMR (125 MHz, DMSO-d_6): 181.7, 170.0, 164.5, 161.4, 157.7, 155.0, 107.1, 103.8, 99.0, 94.0, 76.0, 62.2, 31.8, 31.6, 30.6, 26.2, 18.9, 18.8, 13.8. ESI-MS (m/z): 360.5 [M-H]-.

4.3. Cell lines and viruses

U373-CD4-CCR5 cell line was obtained from the AIDS Research and Reagent Program, NIAID. Cells were cultured according to the protocol of the provider with 10% heat-inactivated fetal bovine serum (Lonza, The Netherlands) supplemented with 2 mM L-glutamine, 100 units/ml of penicillin and 100 µg/ml streptomycin (Invitrogen, Belgium). Pseudotyped viral particules bearing the ADA HIV Env were produced as described previously [25].

EBV-positive BL cell line P3HR1 cells were cultured in RPMI 1640 medium [26,27]. Culture media were supplemented with 10% fetal calf serum. To induce EBV lytic cycle, P3HR1 cells were treated with 3 mM sodium butyrate and 30 nM 12-O-tetradecanoylphobol-13-actetae (TPA) [26,27].

4.4. Anti-HIV testing

Antiviral activity was assessed using a Pseudotype Virus Assay allowing one cycle of viral replication [25]. U373-CD4-CCR5 cells were infected by pseudotyped virus pNL4.3ΔenvLuc-ADA 8 using spinoculation at 1 200g during 2 hours in the presence of compounds and cultured for two consecutive days in the presence of the compounds. After 48h, luciferase activity expressed as Relative Light Units was measured (Luciferase System kit, Promega, The Netherlands). Drug cytotoxicity was evaluated using MTT (3-(4,5-dimethylthiazol-2-yl)-2,5-diphenyltetrazolium

bromide, Sigma, Belgium) 48 hours after incubation with the compounds by measuring A540 and A690 using a POLARstar Omega Plate Reader (BMG Lab Technologies, Belgium) after 48 hours of incubation with the compounds. Value of OD540 - OD690 was calculated.

4.5. Immunoblot analysis of EBV Rta protein

P3HR1 cells were lysed in mRIPA buffer (50 mM Tris-HCl, pH 7.8, 150 mM NaCl, 5 mM EDTA, 0.5 % Triton X-100, 0.5 % NP-40) [26,27]. About 5% of the lysate was loaded to a gel and separated by electrophoresis in 10% SDS-PAGE. Proteins in the gel were electroblotted onto a polyvinylidene difluoride (PVDF) blotting membrane using a Hoefer transfer system. Rta was detected using mouse anti-Rta monoclonal antibody (Argene). α-Tubulin was detected using mouse anti-α-tubulin monoclonal antibody (Abcam). Primary antibodies were detected using horseradish peroxidase-conjugated secondary antibodies (Cell Signaling Technology) and then visualized using SuperSignal West Pico Chemiluminescent substrate (Pierce).

4.6 Cytotoxicity assay

P3HR1 cells (5×10^4) were seeded in wells of a 96-well plate and cultured for 24 h in 100 μL of RPMI 1640 medium containing protoapigenone or its analogs. Then 1% Triton X-100 was added as a negative control. Cytotoxicity was determined by Cell Proliferation Kit I (Roche). An aliquot of 10 μL of the MTT labeling reagent was added to each well and the plate was incubated for 4 h at 37°C. Then 100 μL solubilization solution was added to each well to dissolve insoluble formazan and was incubated overnight. Optical density was measured at 595 nm and 650 nm.

5. Conclusions

As a result of this work, the chemical space of non-cytotoxic protoflavonoids was significantly extended through the preparation of derivatives without the symmetric dienone moiety, such as saturated (hydrogenated or deuterated) B-ring and/or 4′-oxime containing protoflavones. Compound **9** was found to exert a weak antiretroviral activity that, due to the extremely low cytotoxicity of this compound, may still be of interest. Further, three compounds, the isopropyl-, butyl- and propargyl-ether derivatives of protoapigenone were identified to act as potent anti-EBV agents at similar, medium-low nanomolar concentration range as their parent compound **2**. Importantly, protoapigenone 1′-*O*-isopropyl ether demonstrated an order of magnitude lower cytotoxic effect as compared to protoapigenone, that makes compound **6** ca. 2.6-times more selective anti-EBV agent. Therefore, this compound can serve as a possible new lead for the development of safe and effective protoflavone derivatives against the lytic cycle of EBV.

Altogether, as a result of this work it may also be concluded that targeted chemical modifications of the protoflavone B-ring to decrease cytotoxicity represent a valid strategy towards the discovery of new bioactive compounds against pathologies other than cancer.

Supplementary Materials: ^{1}H and ^{13}C NMR spectra, and ESI-MS spectra of the novel compounds **10**-**13** and **15**-**28** are presented as Supplementary Figures S1-S36 (NMR) and Figures S37-S54. Antiretroviral activity of compound **9** is presented as Figure S55, and cytotoxic IC_{50} values for compounds **2**, **6**-**14** and **21**-**28** on U373-CD4-CCR5 cells are presented as Table S1.

Author Contributions: Conceptualization, A.H.; investigation, M.V., G.G., N.K., J.-Y.S., H.C.; resources, F.F., F.-R.C., A.H.; data curation, M.V., N.K.; writing—original draft preparation, M.V., G.G.; writing—review and editing, M.V., N.K., A.H.; supervision, S.B.Ö., C.D., L.-K.C., A.H.; funding acquisition, J.H., A.H.

Funding: This work was funded by the National Research, Development and Innovation Office, Hungary (NKFIH; K119770), the PN-II-PT-PCCA-2013-4-0930, European Cooperation ERA-NET HIVERA contract 11/2016 and NKFIH NN 118176, the Ministry of Human Capacities, Hungary grant 20391-3/2018/FEKUSTRAT, and the EU-funded Hungarian grant EFOP-3.6.1-16-2016-00008.

Conflicts of Interest: The authors declare no conflict of interest. The funders had no role in the design of the study; in the collection, analyses, or interpretation of data; in the writing of the manuscript, or in the decision to publish the results.

References

1. Hunyadi, A.; Martins, A.; Danko, B.; Chang, F.R.; Wu, Y.C. Protoflavones: a class of unusual flavonoids as promising novel anticancer agents. *Phytochem Rev* **2014**, *13*, 69-77, doi:10.1007/s11101-013-9288-2.
2. Danko, B.; Toth, S.; Martins, A.; Vagvolgyi, M.; Kusz, N.; Molnar, J.; Chang, F.R.; Wu, Y.C.; Szakacs, G.; Hunyadi, A. Synthesis and SAR Study of Anticancer Protoflavone Derivatives: Investigation of Cytotoxicity and Interaction with ABCB1 and ABCG2 Multidrug Efflux Transporters. **2017**, *12*, 850-859, doi:10.1002/cmdc.201700225.
3. Stanković, T.; Dankó, B.; Martins, A.; Dragoj, M.; Stojković, S.; Isaković, A.; Wang, H.-C.; Wu, Y.-C.; Hunyadi, A.; Pešić, M. Lower antioxidative capacity of multidrug-resistant cancer cells confers collateral sensitivity to protoflavone derivatives. *Cancer Chemother Pharmacol* **2015**, *76*, 555-565, doi:10.1007/s00280-015-2821-9.
4. Wang, H.C.; Lee, A.Y.; Chou, W.C.; Wu, C.C.; Tseng, C.N.; Liu, K.Y.; Lin, W.L.; Chang, F.R.; Chuang, D.W.; Hunyadi, A., et al. Inhibition of ATR-dependent signaling by protoapigenone and its derivative sensitizes cancer cells to interstrand cross-link-generating agents in vitro and in vivo. *Mol Cancer Ther* **2012**, *11*, 1443-1453, doi:10.1158/1535-7163.mct-11-0921.
5. Lecona, E.; Fernandez-Capetillo, O. Targeting ATR in cancer. *Nature Reviews Cancer* **2018**, *18*, 586-595, doi:10.1038/s41568-018-0034-3.
6. Lin, A.S.; Nakagawa-Goto, K.; Chang, F.R.; Yu, D.; Morris-Natschke, S.L.; Wu, C.C.; Chen, S.L.; Wu, Y.C.; Lee, K.H. First total synthesis of protoapigenone and its analogues as potent cytotoxic agents. *J Med Chem* **2007**, *50*, 3921-3927, doi:10.1021/jm070363a.
7. Hunyadi, A.; Chuang, D.W.; Danko, B.; Chiang, M.Y.; Lee, C.L.; Wang, H.C.; Wu, C.C.; Chang, F.R.; Wu, Y.C. Direct semi-synthesis of the anticancer lead-drug protoapigenone from apigenin, and synthesis of further new cytotoxic protoflavone derivatives. *PLoS One* **2011**, *6*, e23922, doi:10.1371/journal.pone.0023922.
8. Lin, A.S.; Chang, F.R.; Wu, C.C.; Liaw, C.C.; Wu, Y.C. New cytotoxic flavonoids from *Thelypteris torresiana*. *Planta Med* **2005**, *71*, 867-870, doi:10.1055/s-2005-871292.
9. Hunyadi, A.; Martins, A.; Danko, B.; Chuang, D.-W.; Trouillas, P.; Chang, F.-R.; Wu, Y.-C.; Falkay, G. Discovery of the first non-planar flavonoid that can strongly inhibit xanthine oxidase: protoapigenone 1′-O-propargyl ether. *Tetrahedron Lett* **2013**, *54*, 6529-6532, doi:10.1016/j.tetlet.2013.09.087.
10. Tung, C.P.; Chang, F.R.; Wu, Y.C.; Chuang, D.W.; Hunyadi, A.; Liu, S.T. Inhibition of the Epstein-Barr virus lytic cycle by protoapigenone. *J Gen Virol* **2011**, *92*, 1760-1768, doi:10.1099/vir.0.031609-0.
11. Ötvös, S.B.; Vágvölgyi, M.; Girst, G.; Kuo, C.-Y.; Wang, H.-C.; Fülöp, F.; Hunyadi, A. Synthesis of Nontoxic Protoflavone Derivatives through Selective Continuous-Flow Hydrogenation of the Flavonoid B-Ring. *ChemPlusChem* **2018**, *83*, 72-76, doi:10.1002/cplu.201700463.
12. Ko, Y.-J.; Oh, H.-J.; Ahn, H.-M.; Kang, H.-J.; Kim, J.-H.; Ko, Y.H. Flavonoids as potential inhibitors of retroviral enzymes. *Journal of the Korean Society for Applied Biological Chemistry* **2009**, *52*, 321-326, doi:10.3839/jksabc.2009.057.
13. Kurapati, K.R.V.; Atluri, V.S.; Samikkannu, T.; Garcia, G.; Nair, M.P.N. Natural Products as Anti-HIV Agents and Role in HIV-Associated Neurocognitive Disorders (HAND): A Brief Overview. *Front Microbiol* **2016**, *6*, 1444-1444, doi:10.3389/fmicb.2015.01444.

14. Áy, É.; Hunyadi, A.; Mezei, M.; Minárovits, J.; Hohmann, J. Flavonol 7-O-Glucoside Herbacitrin Inhibits HIV-1 Replication through Simultaneous Integrase and Reverse Transcriptase Inhibition. *Evidence-Based Complementary and Alternative Medicine* **2019**, *2019*, 6, doi:10.1155/2019/1064793.
15. Iglesias, J.; Sleno, L.; Volmer, D.A. Isotopic labeling of metabolites in drug discovery applications. *Curr Drug Metab* **2012**, *13*, 1213-1225.
16. Robins, R.J.; Billault, I.; Duan, J.-R.; Guiet, S.; Pionnier, S.; Zhang, B.-L. Measurement of 2H distribution in natural products by quantitative 2H NMR: An approach to understanding metabolism and enzyme mechanism? *Phytochemistry Reviews* **2003**, *2*, 87-102, doi:10.1023/B:PHYT.0000004301.52646.a8.
17. Krumbiegel, P. Large deuterium isotope effects and their use: a historical review. *Isotopes in environmental and health studies* **2011**, *47*, 1-17, doi:10.1080/10256016.2011.556725.
18. Gant, T.G. Using deuterium in drug discovery: leaving the label in the drug. *J Med Chem* **2014**, *57*, 3595-3611, doi:10.1021/jm4007998.
19. Ötvös, S.B.; Hsieh, C.-T.; Wu, Y.-C.; Li, J.-H.; Chang, F.-R.; Fülöp, F. Continuous-Flow Synthesis of Deuterium-Labeled Antidiabetic Chalcones: Studies towards the Selective Deuteration of the Alkynone Core. *Molecules (Basel, Switzerland)* **2016**, *21*, 318-318, doi:10.3390/molecules21030318.
20. Otvos, S.B.; Mandity, I.M.; Fulop, F. Highly selective deuteration of pharmaceutically relevant nitrogen-containing heterocycles: a flow chemistry approach. *Molecular diversity* **2011**, *15*, 605-611, doi:10.1007/s11030-010-9276-z.
21. Hsieh, C.-T.; Ötvös, S.B.; Wu, Y.-C.; Mándity, I.M.; Chang, F.-R.; Fülöp, F. Highly Selective Continuous-Flow Synthesis of Potentially Bioactive Deuterated Chalcone Derivatives. *ChemPlusChem* **2015**, *80*, 859-864, doi:10.1002/cplu.201402426.
22. Kozłowska, J.; Grela, E.; Baczyńska, D.; Grabowiecka, A.; Anioł, M. Novel O-alkyl Derivatives of Naringenin and Their Oximes with Antimicrobial and Anticancer Activity. *Molecules* **2019**, *24*, 679.
23. Türkkan, B.; Özyürek, M.; Bener, M.; Güçlü, K.; Apak, R. Synthesis, characterization and antioxidant capacity of naringenin-oxime. *Spectrochimica Acta Part A: Molecular and Biomolecular Spectroscopy* **2012**, *85*, 235-240, doi:https://doi.org/10.1016/j.saa.2011.09.066.
24. Latif, A.D.; Gonda, T.; Vágvölgyi, M.; Kúsz, N.; Kulmány, Á.; Ocsovszki, I.; Zomborszki, Z.P.; Zupkó, I.; Hunyadi, A. Synthesis and In Vitro Antitumor Activity of Naringenin Oxime and Oxime Ether Derivatives. *International Journal of Molecular Sciences* **2019**, *20*, 2184.
25. Arendt, V.; Amand, M.; Iserentant, G.; Lemaire, M.; Masquelier, C.; Ndayisaba, G.F.; Verhofstede, C.; Karita, E.; Allen, S.; Chevigné, A., et al. Predominance of the heterozygous CCR5 delta-24 deletion in African individuals resistant to HIV infection might be related to a defect in CCR5 addressing at the cell surface. *Journal of the International AIDS Society* **2019**, *22*, e25384, doi:10.1002/jia2.25384.
26. Chang, L.K.; Lee, Y.H.; Cheng, T.S.; Hong, Y.R.; Lu, P.J.; Wang, J.J.; Wang, W.H.; Kuo, C.W.; Li, S.S.; Liu, S.T. Post-translational modification of Rta of Epstein-Barr virus by SUMO-1. *The Journal of biological chemistry* **2004**, *279*, 38803-38812, doi:10.1074/jbc.M405470200.
27. Yang, Y.C.; Yoshikai, Y.; Hsu, S.W.; Saitoh, H.; Chang, L.K. Role of RNF4 in the ubiquitination of Rta of Epstein-Barr virus. *The Journal of biological chemistry* **2013**, *288*, 12866-12879, doi:10.1074/jbc.M112.413393.